Kinetik: Game Technology, Information System, Computer Network, Computing, Electronics, and Control
Journal homepage: http://kinetik.umm.ac.id
ISSN: 2503-2267
Vol. 5, No. 3, August 2020, Pp. 227-234

Reduced overshoot of the electroforming jewellery process using PID

Arie Cahyo Utomo*[1], Ponco Siwindarto[2], Onny Setyawati[3]
Department of Control and Electronic System, Brawijaya University[1, 2, 3]

Article Info

Keywords:
Electroforming, PID Control, Xcos Scilab, State Space

Article history:
Received 28 March 2020
Revised 20 July 2020
Accepted 28 July 2020
Published 31 August 2020

Cite:
Utomo, A., Siwindarto, P., & Setyawati, O. (2020). Reduced Overshoot of The Electroforming Jewellery Process Using PID. Kinetik: Game Technology, Information System, Computer Network, Computing, Electronics, and Control, 5(3). doi:https://doi.org/10.22219/kinetik.v5i3.1059

*Corresponding author.
Arie Cahyo Utomo
E-mail address:
ariecahyo.9294@gmail.com

Abstract

The electroforming jewellery is the electrodeposition process of coating metal on an insulator object to make a jewellery product. The problems are burnt and uneven results in their products, it happened because electrical currents while the process increased. So, too many metal particles attached to object. The problems of electroforming process can fix with a control system, where controller must makes constant electrical currents while the process. In this paper, the problems was changed to the equation by the polynomial regression method as a plant. Secondly the characteristic of current sensor was found by the linier regression method as a feedback system. The system used buck converter as the actuator, where it was written to the equation by the state space method. The controller was chosen by comparison 4 types controller, they are a conventional controller, proportional controller, proportional – integral (PI) controller, and proportional – integral – derivative (PID) controller. Xcos Scilab used to simulated the system and got the system with a proportional – integral – derivative controller is the best controller. The system with a proportional – integral – derivative controller have a Rise time 1.3687×10^{-5} Seconds and Overshoot 2.5420%. The result of research will be base to makes hardware system where it will help the advancement of the creative economy industry in Malang City.

1. Introduction

Generally, the jewellery are made by metals like a from gold, silver, copper, brass, nickel and the others. Certainly, the process make it is many variation, one of them is Electrodeposition. Electrodeposition is a well-known conventional surface modification method to improve the surface characteristics, decorative and functional, of a wide variety of materials [1]. Electrodeposition has 3 types, they are Electroplating, Heavy Deposition and Electroforming [2]. Now in Malang City, most favorite method to makes jewellery is Electroforming.

Electroforming in jewellery is a process of coating metal on an insulator object to make a jewellery product. Electroforming process needs a plating bath. Inside the bath, two electrodes (anode and cathode) are installed at each side to charge the electricity, and the principal parameters of the electroforming process are electric current density, concentration and pH of electrolytes, temperature of plating bath, etc [3]. The insulator object need additional ingredient to makes metal can coating to object, it is a Graphite. Graphite is one of carbon allotropes with hexagonal lattice structure, this layer of carbon has unique electrical and optical properties [4].

Generally, Craftsman of electroforming jewellery in Malang city are using electroforming acid copper solution. They have many failures in their production process, where their jewellery are burnt and uneven results. This problems makes their production cost is increasing. When we saw how they did, they made a process electroforming jewellery with a constant voltage by the power supply voltage. So electric current increased together with time of process. Necessarily, electric current must be constant because electron transfer is considered as the main factor of electroforming [3]. The reason why electric current increased, because the resistance of object decreased by how many copper coated at object, and resistance of graphite is highly then copper resistance.

In this paper, we are answering the problem with a research. Where we compared 4 types controller, there are a conventional controller, proportional controller, proportional – integral controller, and proportional – integral – derivative controller. The actuator used DC – DC converter step down or buck converter for decreased voltage from 12V to 0.1V. The voltage after actuator is adjustable, but electric current can constant because a control system. The buck converter was chosen because it is have a small lost power. In a Buck Converter Circuit there are components such MOSFET as electronic switching, diode, inductor and capacitor [5]. The feedback system used characteristic of sensor ACS712 with linier regression. The ACS712 is a current sensor that provides economical and precise solutions for AC or DC current sensing in industrial, commercial, and communications systems [6]. The plant is electroforming acid copper solution process where it was written by polynomial regression. This research used Xcos Scilab as a platform to simulated and to choose where the best controller for the system.

2. Research Method

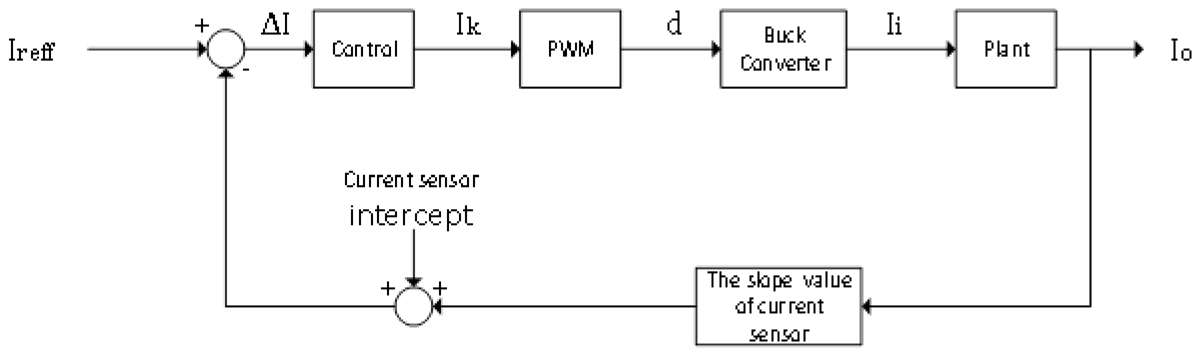

Figure 1. The Block Diagram of System Control in Electroforming Jewellery

If we started from dimension of object which to coating, I_{reff} in Figure 1 are got by Equation 1. The dimension unit of object is using Centimeter and I_{reff} is using Ampere unit. The target system must has Rise time no more than 1 milliseconds and Overshoot value no more than 5%.

$$I_{reff} = \frac{P_b \times L_b}{100} \times 0.5 \quad (1)$$

2.1 Electroforming plant modelling

The modelling of Electroforming acid copper solution based on experiment at object with a constant voltage 2.2V, this experiment aims to find the electric current response while the process. Figure 2 is illustrating the installation of experiment, anode are used for copper material and cathode are used for the object which want to coating. The copper material will move to object when there is a working electromotive force (e.m.f). The electric current response has been written to equation by polynomial regression. Polynomial regression is a special case of multiple regression, with only one independent variable X [7]. Variable X in this experiment is a time of process and Variable Y is the electric current response. The electric current response can be expressed as Equation 2, and constant value $a0 - a10$ are got by matrix in Equation 3. Equation 2 can entered to Equation 4 to know the resistance response while the process.

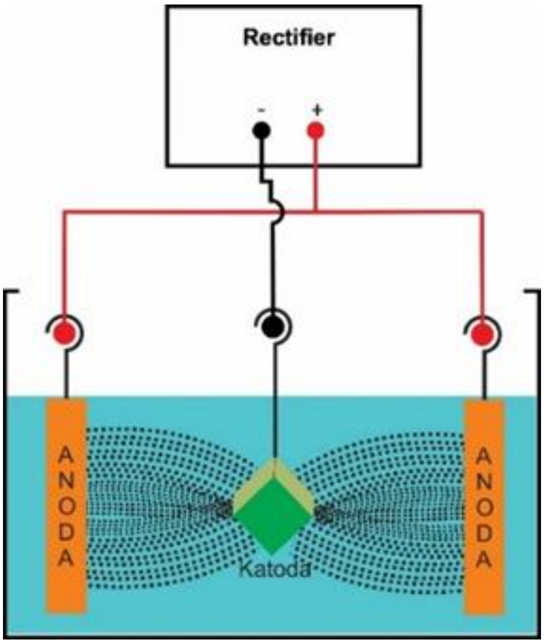

Figure 2. The Electrical Installation of Electroforming Experiment

$$ip(t) = a0 + a1t + a2t^2 + a3t^2 + a4t^2 + a5t^2 + a6t^2 + a7t^2 + a8t^2 + a9t^2 + a10t^2 \quad (2)$$

$$\begin{bmatrix} a0 \\ a1 \\ a2 \\ \vdots \\ a10 \end{bmatrix} = \begin{bmatrix} n & \sum_{i=1}^{n} t_i & \sum_{i=1}^{n} t_i^{\,2} & \cdots & \sum_{i=1}^{n} t_i^{\,10} \\ \sum t_i & \sum_{i=1}^{n} t_i^{\,2} & \sum_{i=1}^{n} t_i^{\,3} & \cdots & \sum_{i=1}^{n} t_i^{\,11} \\ \sum_{i=1}^{n} t_i^{\,2} & \sum_{i=1}^{n} t_i^{\,3} & \sum_{i=1}^{n} t_i^{\,4} & \cdots & \sum_{i=1}^{n} t_i^{\,12} \\ \vdots & \vdots & \vdots & \ddots & \vdots \\ \sum_{i=1}^{n} t_i^{\,10} & \sum_{i=1}^{n} t_i^{\,11} & \sum_{i=1}^{n} t_i^{\,12} & \cdots & \sum_{i=1}^{n} t_i^{\,20} \end{bmatrix}^{-1} \cdot \begin{bmatrix} \sum_{i=1}^{n} ip_i \\ \sum_{i=1}^{n} t_i ip_i \\ \sum_{i=1}^{n} t_i^{\,2} ip_i \\ \vdots \\ \sum_{i=1}^{n} t_i^{\,10} ip_i \end{bmatrix} \quad (3)$$

$$R(t) = \frac{2.2}{ip(t)} \quad (4)$$

2.2 Electric current sensor modelling

The feedback system used characteristic of sensor ACS712 with a linier regression in Equation 6. The linear regression model assumes linear relationship between input variables and output variable [8]. The sensor have a sensitivity $100\frac{mV}{A}$. The characteristic was got by experiment with microcontroller, and it compared with Dekko power supply indicator. Output voltage was changed to electric current by ADC microcontroller with Equation 5. ADC converts an analog input voltage into a digital number so that it can be processed by the microcontroller or any other digital processor [9].

$$I_o = \frac{ADC\ value\ \times\ 5}{sensitivity\ \times\ 1024} \quad (5)$$

$$i_{act} = intercept + (slope\ \times\ I_o) \quad (6)$$

2.3 Buck converter modelling

The inherent switching operation of electronic power converter resulted circuit components which connected in periodic changes together, every configuration was explained by the separate equation. If we are using transient analysis for this buck converter is too difficult, so state space averaging method can be solution for this problem. State space averaging is a common alternating current converter modeling technique and is used in this section to derive the small signal model of the composite converter [10].

The output voltage level at the load is controlled by varying the width of the switch chopped input pulse, which is basically controlling the duration of the time the electronic switches, MOSFETs, are ON or OFF in one cycle of the operating frequency; this is known as pulse width modulation [11]. The MOSFET (metal oxide silicon field effect transistor) is a fast-switching transistor with relatively blocking high voltage that requires very little power to control [12]. Derivative of current inductor and integral capacitor voltage was determined by circuit theory for each substructure. Figure 3(a) is a buck converter circuit which have equivalent circuit when MOSFET is active in Figure 3(b) and the equivalent circuit when MOSFET is not active in Figure 3(c).

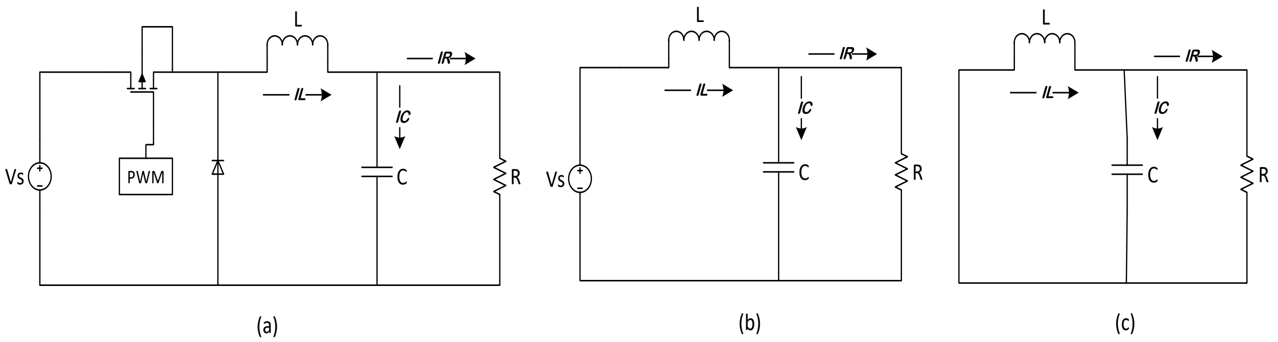

Figure 3. Buck Converter Circuit and Equivalent Circuit

When the MOSFET is active, Equation 8 and Equation 10 is explaining the state space. The equation 8 is explanation from Equation 7, and the Equation 10 is explanation from Equation 9.

$$\dot{x} = A_1 \, x + B_1 \, u \tag{7}$$

$$\begin{bmatrix} \dot{i_L} \\ \dot{v_c} \end{bmatrix} = \begin{bmatrix} 0 & -\frac{1}{L} \\ \frac{1}{C} & -\frac{1}{CR} \end{bmatrix} \begin{bmatrix} i_L \\ v_c \end{bmatrix} + \begin{bmatrix} \frac{1}{L} \\ 0 \end{bmatrix} V_s \tag{8}$$

$$y = C_1 x + D_1 \, u \tag{9}$$

$$\begin{bmatrix} i_R \\ v_R \end{bmatrix} = \begin{bmatrix} 0 & \frac{1}{R} \\ 0 & 1 \end{bmatrix} \begin{bmatrix} i_L \\ v_c \end{bmatrix} + \begin{bmatrix} 0 \\ 0 \end{bmatrix} V_s \tag{10}$$

When the MOSFET is not active, matrix A_2 is equals matrix A_1, and matrix C_2 is equals matrix C_1. The two states are combined in Equation 11 and give Equation 12. So, the averaging state space equation is explanation in Equation 13. The output state has a different in matrix B_2 only, where it has a zero value. Both output states are operated into Equation 14 and produce Equation 15. The averaging state space equation of output in Equation 16. The value's capacitor is 100μF, inductor has value 400μH, Vs or Source voltage is using 50V and frequency of PWM is using 1Hz.

$$\dot{x} = [A_1 xd + A_2 x(1-d)] + [B_1 \, ud + B_2 \, u(1-d)] \tag{11}$$

$$\dot{x} = Ax + Bud \tag{12}$$

$$\begin{bmatrix} \dot{i_L} \\ \dot{v_c} \end{bmatrix} = \begin{bmatrix} 0 & -\frac{1}{L} \\ \frac{1}{C} & -\frac{1}{CR} \end{bmatrix} \begin{bmatrix} i_L \\ v_c \end{bmatrix} + \begin{bmatrix} \frac{V_s}{L} \\ 0 \end{bmatrix} d \tag{13}$$

$$y = [C_1 xd + C_2 x(1-d)] \tag{14}$$

$$y = Cx \tag{15}$$

$$\begin{bmatrix} i_R \\ v_R \end{bmatrix} = \begin{bmatrix} 0 & \frac{1}{R} \\ 0 & 1 \end{bmatrix} \begin{bmatrix} i_L \\ v_c \end{bmatrix} \tag{16}$$

2.4 Xcos Scilab diagram block

SciLab belongs to the software (developed on the base of open and free technologies) that enables to simulate dynamical systems. In its nature it reminds Matlab mainly because of its graphical interface Xcos that is very similar to Simulink [13]. Equation 13 and Equation 16 is shown in Figure 4 and Equation 4 is included in Figure 4. The diagram block of conventional controller is shown in Figure 5, the conventional has 2 output state only: high and low or on and off (on-off controller) and they are used for their simplicity, operation reliability and low cost [14]. The three other controller is shown in Figure 6. When we will analysis response, diagram block of controller will be separated in accordance with the controller will be tested at the time.

Proportional control can be explained as follows: the change in output of the controller is proportional to the input signal produced by the environmental change (commonly referred to as error) which has been detected by a sensor [15]. The gain value from Proportional control is Kp. Sometimes Proportional control has a big steady state error, we can fix it with add the integral controller and the controller to be the proportional – integral control where it has Kp gain value and Ki gain value. The integral controller can effectively eliminate the steady-state error. This is because of the nature of the integral controller producing its output from the accumulated past errors [16][17]. The effect of integral controllers is measured in units of minutes per repeat or its reciprocal, a high number of minutes per repeat indicates a low action by the integral controller [18].

If proportional control and proportional – integral control cannot makes a stability system, PID will be a final solution. The derivative control is used to reduce the magnitude of the overshoot produced by the integral component and to improve process stability [19][20]. So we have Kp, Ki, and Kd for the gain values in PID. The system is changed to s – domain to determine gain Kp, Ki and Kd. The gain values determine using Root locus method. The original function $f(t)$ and its Laplace transform $F(s)$ form a Laplace pair [21][22]. The root locus method allows to determine the specific value of a process parameter for a desired root location, and with it, for a desired dynamic response [23][24][25].

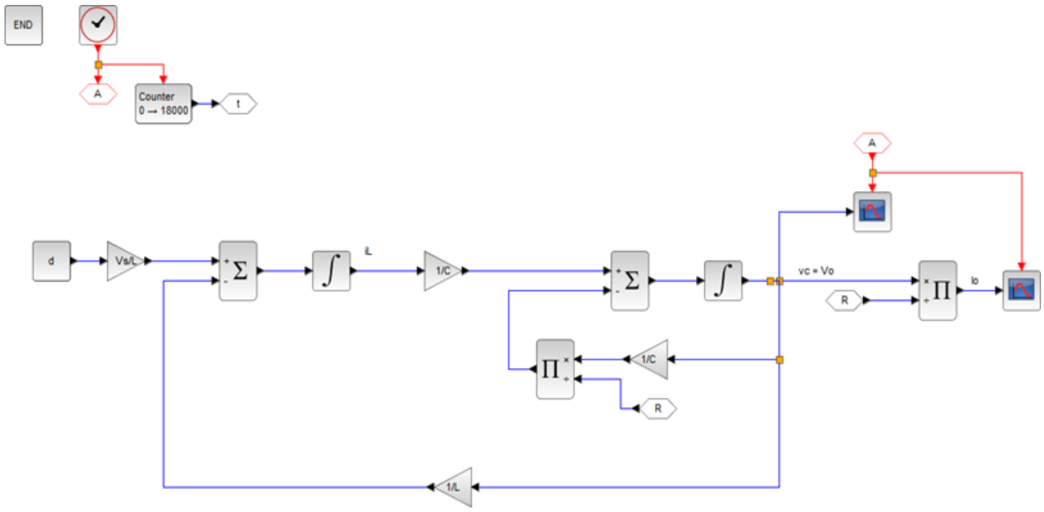

Figure 4. The Diagram Block of State Space Buck Converter and Plant in Xcos Scilab

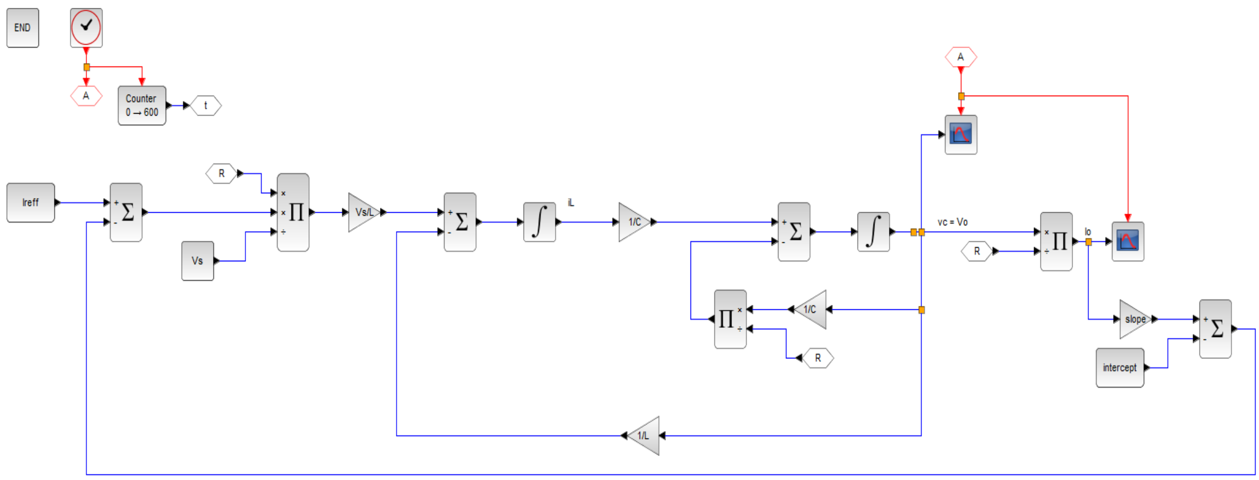

Figure 5. The Diagram Block of System with a Conventional Controller

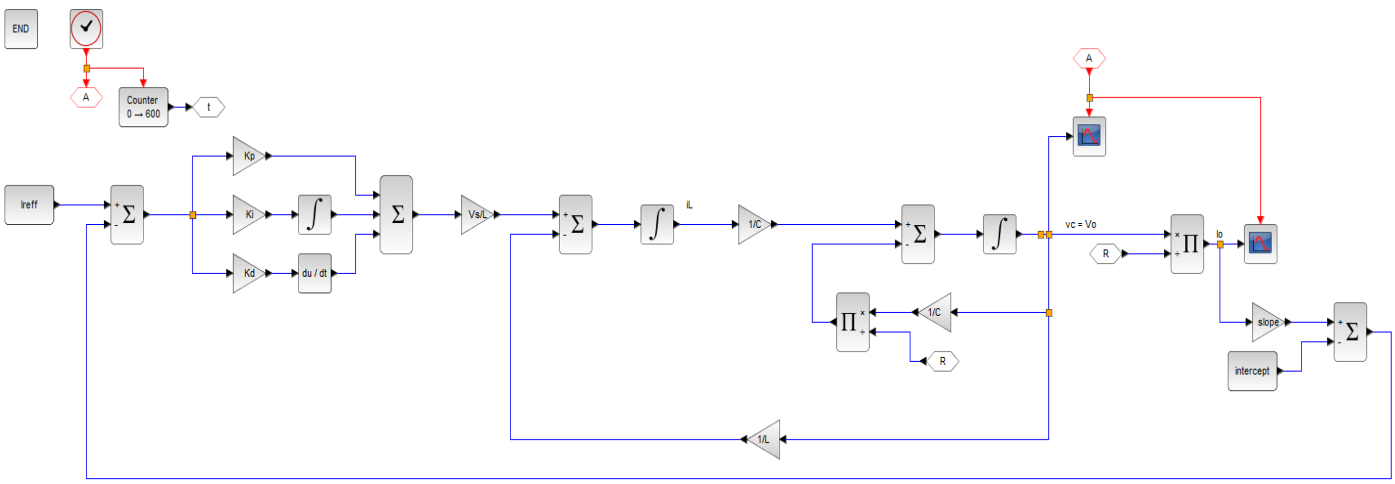

Figure 6. The Diagram Block of System with 3 Controller Types

Cite: Utomo, A., Siwindarto, P., & Setyawati, O. (2020). Reduced Overshoot of The Electroforming Jewellery Process Using PID. Kinetik: Game Technology, Information System, Computer Network, Computing, Electronics, and Control, 5(3). doi:https://doi.org/10.22219/kinetik.v5i3.1059

3. Results and Discussion

The result of electroforming plant modelling is shown in Figure 7. It is clear that resistance value is decreasing while the process, so constant value $a0 - a10$ is shown in Table 1. The result of experiment for feedback of system is represented in Equation 17, where the value of intercept is -0.0284645 and slope value is 1.0092573.

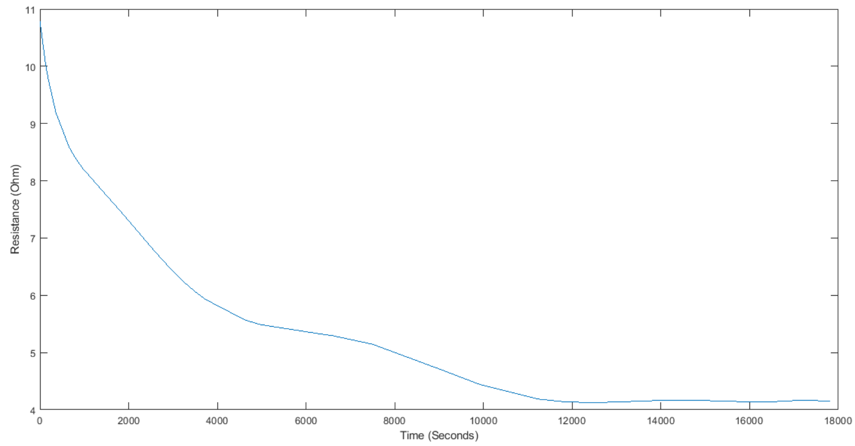

Figure 7. Resistance Response of Plant

Table 1. Constant Value of Polynomial Regression

Variable	Value	Variable	Value
$a0$	0.2038845091155963	$a6$	-2.7288300966979393E-22
$a1$	1.3325461753765921E-4	$a7$	1.5056912794092627E-26
$a2$	-1.1639941166485812E-7	$a8$	-4.601807005661936E-31
$a3$	6.368637897862656E-11	$a9$	6.4970385836948E-36
$a4$	-1.8143128781046163E-14	$a10$	-2.0318886576297705E-41
$a5$	2.9038422588505522E-18		

$$i_{act} = -0.0284645 + 1.0092573 I_o \tag{17}$$

The results of modeling are written to S – domain by Laplace transform and it based diagram block in Figure 1. So, the transfer function of system is shown in Equation 18. The best gain of P control, PI control and PID control is shown in Table 2, the gain values has been got by root locus with Equation 18 each controller types. When we searched the gain for P control, small value gain of Kp is makes the response cannot reach a current references. But if value gain of Kp is too high, the response to be oscillation. So P control is not good choice for this system. In PI Control, value of Kp is decreased and Ki is increased. But the consequences the rise time to be slowly. In PID control we can got the fast rise time, but the problem on overshoot only.

$$G(s) = \frac{2.5 \times 10^8 s^2 + 2.083 \times 10^{12} s + 6.25 \times 10^{15}}{1.028 s^4 + 1.714 \times 10^4 s^3 + 3.752 \times 10^8 s^2 + 2.531 \times 10^{12} s + 6.951 \times 10^{15}} \tag{18}$$

Table 2. The constant values of 3 type controllers

Name of control	Values
P Control	Kp = 45.6301
PI Control	Kp = 14.5 Ki = 1.55× 10^4
PID Control	Kp = 8.09 Ki = 2.75× 10^4 Kd = 0.000597

Every controllers was tested by step function, and we got a different responses each system. The system with conventional control was got Rise time 7.7391× 10^{-5} Second and Overshoot 43.8989%. P control in system has Rise time 1.0141$\times 10^{-5}$ Seconds and Overshoot 88.3663%. The PI control has Rise time 1.8334 $\times 10^{-5}$ Seconds and Overshoot 81.7260%, and PID control has Rise time 1.3687$\times 10^{-5}$ Seconds and Overshoot 2.5420%. The output responses each controller can see in Figure 8.

So, we can get that PID control is the best controller for the system. Now, input variation is given to see system can makes constant electric current or not. The simulation based on Figure 6, with I_{reff} 0.5A, 1.5A, 2.5A, 3.5A, and 4.5A. The result of simulation is shown in Figure 9, the output voltage changes to adjust the current value to be the same as the current reference value while the process. When in I_{reff} 0.5A, the output voltage maximum reached 5.3V. In I_{reff} 1.5A, the output voltage reached 15.1V for the maximum value. In I_{reff} 2.5A, the maximum of output voltage is measured 23.9V. In I_{reff} 3.5A, we got the maximum of output voltage 32.3V. And I_{reff} 4.5A, we got the maximum of output voltage 41.1V. So if we will make the hardware system with speciation can controlling current until 5A, we must need make the component can handle more than 50V and 5A. So the hardware can handle the overshoot of system and not get damaged quickly.

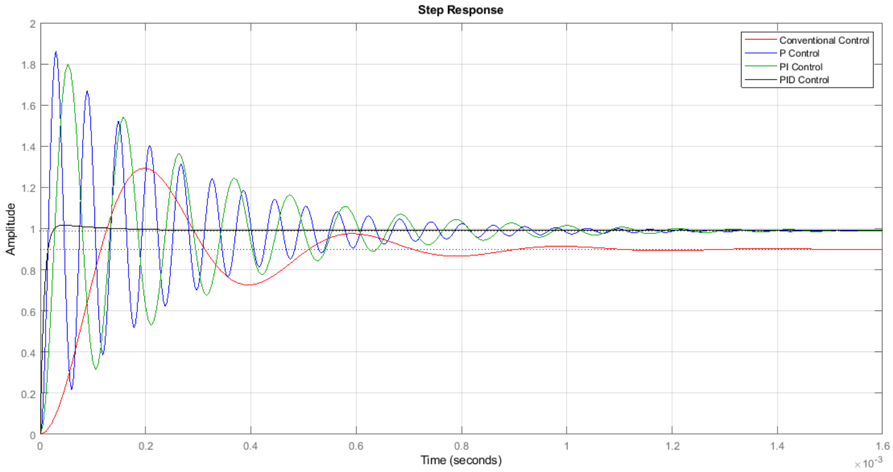

Figure 8. The Output Step Response Each Controller Types

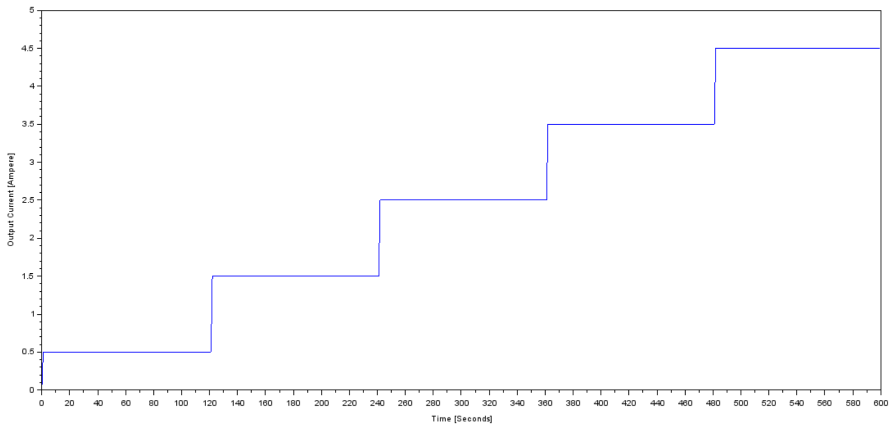

Figure 9. The Result of Simulation System with PID Control Using Xcos Scilab

4. Conclusion

The electroforming jewellery process has the electric current response directly proportional with time and how much copper metals attached in object. All control system has Rise time value below the target, but only PID control reaches the target of overshoot where there has Rise time 1.3687$\times 10^{-5}$ Seconds and Overshoot 2.5420%. The system with PID control tested in Xcos Scilab and we got the system can made the current constant while the process. This result can be the best option for next research about making power supply hardware to controlling electric current in electroforming jewellery process.

Notation

P_b = The length of the object
L_b = The width of the object

I_{reff}	= Electric current reference
$ip(t)$	= Electric current plant function
t	= Time
$a0 - a10$	= The Constant value of polynomial regression
i_{act}	= The actual current from ACS712 sensor
I_o	= The output current in system
$R(t)$	= Resistance plant function
d	= duty cycle
C	= Capacitor's value
L	= Inductor's value
V_s	= The voltage source value
$G(s)$	= The transfer function of system with conventional control
n	= The quantity of data

Acknowledgement

Thanks to CV. Silver 999, Electroforming Jewellery Community Chapter Malang, and Brawijaya University because their help to this research.

References

[1] D. Sobha Jayakrishnan, "Electrodeposition: the versatile technique for nanomaterials," *Corros. Prot. Control Using Nanomater.*, Pp. 86–125, Jan. 2012, https://doi.org/10.1533/9780857095800.1.86
[2] Leslie Curtis, *Electroforming Jewellery Handbooks*. London: A&C Black Publisher Ltd, 2004.
[3] C.-W. Park and K.-Y. Park, "An effect of dummy cathode on thickness uniformity in electroforming process," *Results Phys.*, Vol. 4, Pp. 107–112, Jan. 2014, https://doi.org/10.1016/j.rinp.2014.07.004
[4] Y. Mahmoodi and D. Fathi, "Interaction of TM/ TE waves with graphite and MWCNT photonic crystals," 2016, Pp. 1805–1808, https://doi.org/10.1109/IranianCEE.2016.7585814
[5] A. W. Cristri and R. F. Iskandar, "Analysis and Design of Dynamic Buck Converter with Change in Value of Load Impedance," *Procedia Eng.*, Vol. 170, Pp. 398–403, Jan. 2017, https://doi.org/10.1016/j.proeng.2017.03.064
[6] K. M. E. Galera and O. E. Llantos, "Mobile Web Energy Monitoring System Using DFRduino Uno," *Procedia Comput. Sci.*, Vol. 124, Pp. 706–713, Jan. 2017, https://doi.org/10.1016/j.procs.2017.12.208
[7] E. Ostertagová, "Modelling using Polynomial Regression," *Procedia Eng.*, Vol. 48, Pp. 500–506, Jan. 2012, https://doi.org/10.1016/j.proeng.2012.09.545
[8] Y.-S. Kim, S. Seok, J.-S. Lee, S. K. Lee, and J.-G. Kim, "Optimizing anode location in impressed current cathodic protection system to minimize underwater electric field using multiple linear regression analysis and artificial neural network methods," *Eng. Anal. Bound. Elem.*, Vol. 96, Pp. 84–93, Nov. 2018, https://doi.org/10.1016/j.enganabound.2018.08.012
[9] D. Ibrahim, "Intermediate Level Projects," *Arm-Based Microcontroller Proj. Using Mbed*, Pp. 135–259, Jan. 2019, https://doi.org/10.1016/B978-0-08-102969-5.00008-2
[10] F. Schultheis and D. Maksimovic, "Modeling and control of a step-down composite DC-DC converter," 2015, Pp. 1–6, https://doi.org/10.1109/COMPEL.2015.7236499
[11] M. H. Rashid, A. A. Abu-aisheh, and M. G. Batarseh, "DC–DC converters," *Electr. Renew. Energy Syst.*, Pp. 337–353, Jan. 2016, https://doi.org/10.1016/B978-0-12-804448-3.00015-3
[12] V. I. Rudnev and D. Loveless, "Induction Hardening: Technology, Process Design, and Computer Modeling," *Compr. Mater. Process.*, Pp. 489–580, Jan. 2014, https://doi.org/10.1016/B978-0-08-096532-1.01217-6
[13] Z. Magyar and K. Žáková, "SciLab Based Remote Control of Experiments," *IFAC Proc. Vol.*, Vol. 45, No. 11, Pp. 206–211, Jan. 2012, https://doi.org/10.3182/20120619-3-RU-2024.00099
[14] T. Uriča and A. Simonová, "Simulation of an on-off Controller for Systems of Second Order with the Use of LabVIEW," *Procedia Eng.*, vol. 192, Pp. 905–910, Jan. 2017, https://doi.org/10.1016/j.proeng.2017.06.156
[15] P. F. Stanbury, A. Whitaker, S. J. Hall, P. F. Stanbury, A. Whitaker, and S. J. Hall, "Instrumentation and control," *Princ. Ferment. Technol.*, Pp. 487–536, Jan. 2017, https://doi.org/10.1016/B978-0-08-099953-1.00008-9
[16] S.-H. Kim, "Control of direct current motors," *Electr. Mot. Control*, Pp. 39–93, Jan. 2017, https://doi.org/10.1016/B978-0-12-812138-2.00002-7
[17] W. Bolton, "Process Controllers," *Instrum. Control Syst.*, Pp. 99–121, Jan. 2015, https://doi.org/10.1016/B978-0-08-100613-9.00005-5
[18] P. Bajpai, "Process Control," *Biermann's Handb. Pulp Pap.*, Pp. 483–492, Jan. 2018, https://doi.org/10.1016/B978-0-12-814238-7.00024-6
[19] K. L. S. Sharma, "Automation Strategies," *Overv. Ind. Process Autom.*, Pp. 53–74, Jan. 2017, https://doi.org/10.1016/B978-0-12-805354-6.00006-2
[20] M. Krarti, "Control Strategies for Building Energy Systems," *Optim. Des. Retrofit Energy Effic. Build. Communities, Urban Centers*, Pp. 117–187, Jan. 2018, https://doi.org/10.1016/B978-0-12-849869-9.00003-X
[21] X.-S. Yang, "Laplace Transforms," *Eng. Math. with Examples Appl.*, Pp. 187–198, Jan. 2017, https://doi.org/10.1016/B978-0-12-809730-4.00022-7
[22] V. Magnasco, "Special functions," *Elem. Mol. Quantum Mech.*, Pp. 151–214, Jan. 2013, https://doi.org/10.1016/B978-0-444-62647-9.00004-X
[23] Y. Bavafa-Toosi and Y. Bavafa-Toosi, "Root locus," *Introd. to Linear Control Syst.*, Pp. 377–467, Jan. 2017, https://doi.org/10.1016/B978-0-12-812748-3.00005-7
[24] M. A. Haidekker, "The Root Locus Method," *Linear Feed. Control.*, Pp. 175–191, Jan. 2013, https://doi.org/10.1016/B978-0-12-405875-0.00012-7
[25] A. Visioli, M. S. Fadali, and A. Visioli, "Analog Control System Design," *Digit. Control Eng.*, Pp. 127–164, Jan. 2013, https://doi.org/10.1016/B978-0-12-394391-0.00005-8